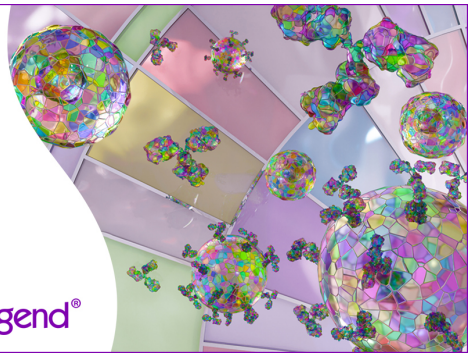

The Journal of Immunology
RESEARCH ARTICLE | MARCH 20 2023

Mast Cell Proteases Cleave Prion Proteins and a Recombinant Ig against PrP Can Activate Human Mast Cells FREE

Steven D. Willows; ... et. al

J Immunol (2023) 210 (9): 1447–1458.
https://doi.org/10.4049/jimmunol.2200726

Mast Cell Proteases Cleave Prion Proteins and a Recombinant Ig against PrP Can Activate Human Mast Cells

Steven D. Willows,* Valentyna Semenchenko,* Grant Norman,[†,‡] Michael T. Woodside,[‡,§,¶] Valerie L. Sim,[†,‡] and Marianna Kulka*[,‖]

IgE Abs, best known for their role in allergic reactions, have only rarely been used in immunotherapies. Nevertheless, they offer a potential alternative to the more commonly used IgGs. The affinity of IgE Ag binding influences the type of response from mast cells, so any immunotherapies using IgEs must balance Ag affinity with desired therapeutic effect. One potential way to harness differential binding affinities of IgE is in protein aggregation diseases, where low-affinity binding of endogenous proteins is preferred, but enhanced binding of clusters of disease-associated aggregated proteins could target responses to the sites of disease. For this reason, we sought to create a low-affinity IgE against the prion protein (PrP), which exists in an endogenous monomeric state but can misfold into aggregated states during the development of prion disease. First, we determined that mast cell proteases tryptase and cathepsin G were capable of degrading PrP. Then we engineered a recombinant IgE Ab directed against PrP from the V region of a PrP-specific IgG and tested its activation of the human mast cell line LAD2. The αPrP IgE bound LAD2 through Fc receptors. Crosslinking receptor-bound αPrP IgE activated SYK and ERK phosphorylation, caused Fc receptor internalization, and resulted in degranulation. This work shows that a recombinant αPrP IgE can activate LAD2 cells to release enzymes that can degrade PrP, suggesting that IgE may be useful in targeting diseases that involve protein aggregation. *The Journal of Immunology*, **2023, 210: 1447–1458.**

IgE is known for initiating allergic inflammation, but it can also activate immune protection from toxins, venoms, and parasites (1). By binding to surface high-affinity IgE receptors (FcεRI), IgE can activate granulated effector cells such as mast cells, basophils, and eosinophils (2). When activated, mast cells release the preformed contents of their granules, which include high concentrations of histamine, proteases, proteoglycans, and other signaling molecules, such as newly synthesized lipid mediators and cytokines/chemokines (2, 3). The proteases released by mast cells include chymase, tryptase, cathepsins, and carboxypeptidase, which can cleave a large variety of target proteins, including blood-clotting factors, cell adhesion proteins, cytokines, and chemokines (4). Some of these proteases are mast cell specific and are not produced by any other immune cell. Although mast cells can be activated by various mechanisms, one of the most specific stimuli in vivo is through clustering of their surface FcεRI receptors by crosslinking of IgE bound to Ag.

Although the IgG class of Abs has seen extensive use as therapeutics for other diseases and are in clinical use (5), IgE has been relatively underused. IgEs have several attributes that could be advantageous in immunotherapy of diseases that are unresponsive to IgG immunotherapy. First, they can overcome immunotolerance, as shown by their role in allergic responses to normally innocuous Ags (6). IgEs generate a strong, self-perpetuating immune response sustained by FcεRI-expressing immune cells (7). The proteases released from effector cells could potentially degrade disease-causing substances or aggregates, whereas effector-released cytokines could recruit other immune cells to disease sites. Moreover, IgEs function best at the mucosal lining of the gastrointestinal tract, whereas IgG functions best in the circulation. IgEs are effective at clearing mucosa-associated pathogens, such as helminths (8), and have been proposed in cancer treatment because some animal model systems have shown that IgE to cancer biomarkers may trigger immune responses that can target and kill tumors (9–11). IgG cannot easily access most solid tissues (12), including brain (13), and it is most often associated with acute and transient humoral immune responses rather than chronic and sustained cellular responses, which would be more appropriate for addressing chronic diseases (11). Furthermore, activation of mast cells via FcεRI requires multiple epitopes in close proximity to crosslink the IgE receptor (14), possibly enabling discrimination between low concentrations of self-antigens present in healthy cells and higher concentrations, or aggregates, of self-antigens present in some diseases.

One reason for the relative underuse of IgE is fear of anaphylaxis. IgE is often involved in allergic reactions, and even small amounts of Ag can induce potentially fatal reactions if enough effector cells are induced to degranulate (15). For example, in a phase 1 human trial of IgE directed against solid tumors expressing folate receptor-α, the IgE was relatively well tolerated but induced anaphylaxis in 1 of the 24 patients (16). For this reason, the binding affinity of any therapeutic IgEs will require fine-tuning to balance the ability of the IgE to bind its Ag and its ability to induce widespread degranulation. Ultimately, low-affinity IgEs may prove useful in therapy because they can induce different immune responses from high-affinity IgEs. For example, in mouse mast cells, a low-affinity stimulus of IgE caused a shift of signaling from the adapter LAT1 to

*Nanotechnology Research Centre, National Research Council Canada, Edmonton, Alberta, Canada; [†]Department of Medicine–Division of Neurology, University of Alberta, Edmonton, Alberta, Canada; [‡]Centre for Prions & Protein Folding Diseases, University of Alberta, Edmonton, Alberta, Canada; [§]Department of Physics, University of Alberta, Edmonton, Alberta, Canada; [¶]Li Ka Shing Institute of Virology, University of Alberta, Edmonton, Alberta, Canada; and [‖]Department of Medical Microbiology and Immunology, University of Alberta, Edmonton, Alberta, Canada

ORCIDs: 0000-0002-1383-478X (S.D.W.); 0000-0003-4695-0397 (M.T.W.); 0000-0002-0088-8666 (V.L.S.); 0000-0003-4741-9290 (M.K.).

Received for publication October 3, 2022. Accepted for publication February 23, 2023.

This work was supported by the National Research Council Canada through the NanoInitiative Program, Canadian Institutes of Health Research Grant MOP-142449 (M.T.W.).

Address correspondence and reprint requests to Dr. Marianna Kulka, University of Alberta, 11421 Saskatchewan Drive, Edmonton, AB T6G 2A3, Canada. E-mail address: marianna.kulka@nrc-cnrc.gc.ca

Abbreviations used in this article: FSC, forward scatter; PrP, prion protein; recPrP(29-231), lyophilized hamster prion protein sequence 29-231; RT-QuIC, real-time quaking-induced conversion.

www.jimmunol.org/cgi/doi/10.4049/jimmunol.2200726

related adapter LAT2, resulting in less degranulation, less leukotriene and cytokine production, but higher chemokine production (17). In vivo, this low-affinity Ag also induced less vascular permeability and changed the ratio of recruited monocytes/macrophages to neutrophils. Interestingly, low-affinity IgEs can induce degranulation of mast cells if they are exposed to Ags with multiple epitopes in close proximity (18). Potentially, targeted degranulation via IgE could be used in diseases where the disease state of an endogenous protein involves high local expression or clustering of normally monomeric epitopes, such as in protein misfolding aggregation diseases.

There exist several proteinopathies that involve toxic aggregation of misfolded endogenous proteins, including amyloid-β and τ proteins in Alzheimer's disease, α-synuclein in Parkinson's disease, and TAR DNA-binding protein 43 in amyotrophic lateral sclerosis (19). The hallmark protein folding diseases are the transmissible spongiform encephalopathies, or "prion diseases," which include scrapie in sheep, bovine spongiform encephalopathy in cows, chronic wasting disease in cervids, and Creutzfeldt-Jakob disease in humans (20, 21). Prion diseases are caused by the formation of misfolded isoforms of the endogenously expressed glycoprotein prion protein (PrP). Although PrP in its native cellular form (denoted PrP^{C}) is largely α-helical, it can also exist in β-sheet-rich conformations (denoted PrP^{Sc}) that are prone to aggregation and function as an unusual type of infectious agent that is able to spread disease by converting PrP^{C} molecules into more PrP^{Sc} (22). In transmissible prion diseases, PrP^{Sc} is primarily acquired orally, traveling from the gut through the enteric nervous system to the brain, where it causes progressive neurodegeneration. Although some evidence exists for the involvement of mast cells in proteinopathies, their role in these diseases is not well understood (23, 24). Ultimately, these diseases are invariably fatal with no disease-modifying treatments (25).

For the present study, we have developed an engineered Ab in which we have inserted the V region from an αPrP IgG into the C region of a human IgE to produce a chimeric αPrP IgE. The recombinant αPrP Ab binds surface FcεRI on LAD2 cells and activates phosphorylation of SYK and ERK. When the αPrP Ab is cross-linked, it initiates LAD2 degranulation and the release of proteases, such as tryptase and cathepsin G, that can digest PrP. This work provides evidence that an engineered αPrP IgE can activate mast cells through FcεRI and generate responses that could potentially degrade PrP.

Materials and Methods

Cell lines and media

LAD2 cells were maintained in StemPro-34 serum-free medium (Fisher Scientific) with 20 mM L-glutamine (Fisher Scientific), 500 U/ml penicillin-streptomycin (Fisher Scientific), and 100 ng/ml of stem cell factor (PeproTech). LAD2 cells were a gift from Dr. Arnold Kirschenbaum and Dr. Dean Metcalfe at the National Institute of Allergy and Infectious Diseases, National Institutes of Health.

PrP 45-95 peptide

A peptide representing aa 45 to 95 of human PrP was synthesized by the Alberta Proteomics and Mass Spectrometry Facility in Edmonton, AB, Canada.

Preparation of PrP fibrils

Recombinant deer PrP was expressed and purified as previously described (26). Lyophilized recombinant PrP was dissolved in 6 M guanidine hydrochloride (GdnHCl) at a protein concentration of 5 mg/ml and stored at −80°C. Fibrils were aggregated using a modified real-time quaking-induced conversion (RT-QuIC). The sample was diluted in RT-QuIC buffer (20 mM sodium phosphate, pH 7.4; 130 mM NaCl; 10 mM EDTA; 0.002% SDS) to a final protein concentration of 0.2 mg/ml and 0.2 M GdnHCl. The RT-QuIC was carried out in 96-well plates (white plate, clear bottom; Costar 3610) sealed with thermal adhesive film. The samples were incubated in the presence of 10 mM thioflavin T at 42°C with cycles of 1 min shaking (700 rpm double orbital) and 1 min rest. Thioflavin T fluorescence measurements (450+/210-nm excitation and 480+/210-nm emission; bottom read) confirmed fibril formation.

Digestion of PrP by mast cell enzymes

Recombinant human proteinases carboxypeptidase A1, cathepsin C, granzyme B, and chymase 1 were purchased from the Sino Biological. Cathepsin G from human leukocytes and human lung tryptase were purchased from the Sigma-Aldrich Canada Co. Recombinant hamster prion protein was from Syntheteq Labs. Lyophilized hamster prion protein sequence 29-231 [recPrP(29-231)] or lysozyme (Sigma-Aldrich) was resuspended in 20 mM Tris buffer, pH 7.2, to a concentration of 1 mg/ml, and 15 μg was combined with the following amount of enzymes and gently mixed by pipetting: 0.25 μg carboxypeptidase A1, 0.3 μg cathepsin C, 0.3 μg granzyme B, 0.32 μg chymase 1, 0.5 U cathepsin G, and 0.05 U tryptase. All samples were incubated at 37°C for 2.5 h, then combined with protein gel loading buffer (0.25 M Tris, 10% SDS, 50% glycerol, 0.5 M fresh DTT, 0.25% bromophenol blue, pH 6.8) and incubated at 95°C for 10 min. Next, protein samples were loaded onto a 20% acrylamide gel. After SDS-PAGE, gels were stained with 1% Coomassie Brilliant Blue G-250 and then destained with a solution containing 30% ethanol and 10% acetic acid.

Mast cell supernatant was generated by suspending LAD2 cells at a concentration of 8×10^6 cells/ml in HEPES buffer and exposing to 100 μg/ml of compound 48/80 for 30 min at 37°C. Cells were then pelleted by centrifugation, and supernatant containing expelled granule contents was collected. A quantity of 10 μg of recPrP(29-231) was exposed to 2 or 4 μl of degranulated mast cell supernatant for 1 h at 37°C, and the resulting solution was analyzed by Western blotting with an anti-prion IgG Ab, Sha31 (Cedarlane, catalog no. A03213). Proteinase K was used as a positive control for digestion.

Recombinant Ab construction

pVITRO1-anti-PrP IgE/k mammalian expression vector was constructed by cloning of the L and H chains into the dual Ab expression cassette in pVITRO1. dsDNA fragments corresponding to the 3B5 VL and 13F10 VH sequences from two αPrP IgGs (27) were designed to be inserted between the BspEI/XbaI and AgeI/SalI restriction sites in pVITRO1-dV-IgE/k carrier. Both fragments and all DNA primers were purchased from Integrated DNA Technologies. After PCR amplification and agarose gel purification, 3B5 VL and 13F10 VH segments were introduced into the vector sequentially using the restriction sites indicated above. Correct insertion was verified by DNA sequencing.

Recombinant Ab production

Recombinant αPrP IgE was expressed in the FreeStyle 293-F cell line. Cells were grown in FreeStyle 293 Expression Medium and transfected with expression plasmid using FreeStyle MAX reagent (Invitrogen) according to the manufacturer's protocols. Growing temperature was reduced to 33°C, incubator platform rotating speed was lowered to 110 rpm 24 h after transfection, and incubation was carried out for 9 d. Expressed recombinant Abs were purified from the medium using CHT chromatography and CHT type I 40-μm resin (Bio-Rad Laboratories), which was equilibrated with 25 mM Tris, 3 mM sodium phosphate, pH 7.4. The collected fractions containing recombinant αPrP IgE protein were combined, and buffer was changed to PBS, pH 7.4, by dialysis for 24 h with three buffer changes at 4°C. Samples were concentrated at 4°C using Amicon ultracentrifugation filters with 100 kDa molecular mass cutoff membranes. Glycerol was added to the sample to 50% final concentration (v/v). Recombinant mAb was aliquoted and stored at −20°C. To determine the concentration of the IgE in the samples, an IgE Human ELISA Kit (Invitrogen) was used according to the manufacturer's instructions. Ab stocks were analyzed by SDS-PAGE and staining with Coomassie blue.

Determination of αPrP IgE binding to PrP Ag via Western blot analysis

A quantity of 10 μg of full-length sequence 23-231 recombinant mouse PrP was diluted in radioimmunoprecipitation assay lysis buffer (150 mM NaCl, 1% Triton X-100, 0.5% sodium deoxycholate, 0.1% SDS, 50 mM Tris, pH 8.0). Sample buffer (62.5 mM Tris-HCl; pH 6.8, 5% glycerol, 5% SDS [$NaDodSO_4$], 3 mM EDTA, 0.02% bromophenol blue, 4% β-mercaptoethanol) was then added. Anti-PrP IgE, rPrP, or 10 μg of 10% (w/v) human, mouse, and deer brain homogenates were then boiled at 100°C for 10 min and loaded into a precast NuPAGE 4–12% Bis-Tris gradient gel (Fisher Scientific, catalog no. NP0321BOX). Immunoblots were run in a Novex Mini-Cell apparatus with NuPAGE MES running buffer (Fisher Scientific, catalog no. NP0002) at 150 V for 1 h. Gels were then transferred to a polyvinylidene fluoride membrane (Fisher Scientific, catalog no. IPFL00010) with transfer buffer (1.9 M glycine and 245 mM Tris base) in a Novex XCELL II blot module at 30 V for 45 min. Membranes were probed by diluting the

αPrP IgE in TBS-Tween (0.05%) at 1:500 overnight at 4°C. Membranes were washed for 5 min three times with TBST (0.05%), and then the appropriate alkaline phosphatase–conjugated secondary α-human IgE (Invitrogen, A18793) was added at a dilution of 1:1000 in 5% nonfat skim milk and incubated at room temperature for 1 h. Membranes were washed with TBST (0.01%) three times for 5, 10, and 15 min. After washing, membranes were developed using the Attophos System (Fisher Scientific, catalog no. S1000) for 5 min, then dried before imaging (ImageQuant3000).

Detecting IgE binding by flow cytometry

LAD2 cells were concentrated to a density of 5×10^5 cells/ml and incubated overnight with 100 ng/ml of αPrP IgE, commercial human IgE (clone HE1, Invitrogen), or no Ab. The next day, cells were labeled with an anti-human IgE allophycocyanin Ab for 30 min at 4°C, and fluorescence was analyzed with a CytoFLEX flow cytometer (Beckman Coulter). Cells were distinguished from debris by gating on a subset of cells on a side scatter versus forward scatter (FSC) dot plot, then single cells were selected on a FSC area versus FSC height dot plot.

To determine the specificity of IgE binding to FcεRI, aliquots of αPrP IgE (200 ng/ml) or commercial human IgE (HE1) (200 ng/ml) were preincubated for 1 h at 37°C in media with 1 mg/ml of omalizumab (Genentech). The IgE-omalizumab mixture was then mixed 1:1 with LAD2 cells (1×10^6 cells/ml) and incubated for another 1 h at 37°C. LAD2 cells were washed with 0.1% BSA in PBS and then labeled with α-human IgE allophycocyanin and analyzed by flow cytometry (CytoFLEX, Beckman Coulter). All presented histograms are from individual representative experiments.

Degranulation assay

LAD2 degranulation was determined by β-hexosaminidase release as previously described (28). LAD2 cells were seeded into 12-well plate wells at a density of 5×10^5 cells/ml in complete media and exposed to 0, 1, 5, or 25 ng/ml of control IgE (HE1) or αPrP IgE overnight. After being washed once, cells were resuspended in HEPES buffer (10 mM HEPES, 137 mM NaCl, 2.7 mM KCl, 0.4 mM Na_2HPO_4, 5 mM glucose, 1.8 mM $CaCl_2$, 1.3 mM $MgSO_4$, 0.4% BSA, pH 7.4) and aliquoted at 2.5×10^4 cells/well into a round-bottomed 96-well plate. Each IgE exposed condition was then exposed, in duplicate or quadruplicate, to HEPES buffer alone, 10 μg/ml of goat anti-human IgE (Fisher Scientific), 10 μg/ml of PrP fibrils, or 100 μg/ml of compound 48/80 (MilliporeSigma) for 30 min at 37°C in a 5% CO_2 incubator. For experiments with PrP fibrils, cells were exposed to the above conditions for 60 min. Cells were pelleted, and half the supernatant (50 μl) was transferred to another flat-bottomed 96-well plate. The cell pellet was then lysed by adding 50 μl of 0.1% Triton X-100 and pipetting up and down before being transferred to another flat-bottomed 96-well plate. A quantity of 50 μl of 1 mM pNAG (Sigma-Aldrich) in citrate buffer (0.04 M citric acid, 0.02 M Na_2HPO_4, pH 4.5) was added to both supernatant and lysate wells, and plates were incubated at 37°C for 1.5 h. The reaction was quenched by adding 50 μl of 0.4 M glycine, pH 10.7, and read immediately on a plate reader at 405 nm, with 570 or 530 nm used as a reference. Statistical analysis was done using multiple *t* tests and the Holm-Sidak method to adjust *p* values for multiple comparisons.

Detection of biomarker expression by flow cytometry

LAD2 cells were sensitized overnight with 25 ng/ml of human myeloma control IgE or αPrP IgE. Cells were then washed and exposed 10 μg/ml of αIgE or the indicated concentrations of PrP 45-95 for 24 h. Cells were collected, resuspended in 0.4% BSA/PBS, and labeled with αFcεRI-FITC (eBioscience; 5 μg/ml), αCD29-PE (eBioscience; 12 μg/ml), αC3aR-PE (BD Biosciences; 5 μg/ml), or αCD203c (BD Biosciences; 10 μg/ml) for 1 h at 4°C in the dark. Cells were washed twice with ice-cold 0.1% BSA/PBS and analyzed on a CytoFLEX flow cytometer. Presented histograms are from a single representative experiment.

Detection of changes to surface FcεRI levels by flow cytometry

LAD2 cells were sensitized with 25 ng/ml of commercial control IgE (HE1), αPrP IgE, or no IgE overnight. The next day, cells were washed and resuspended in HEPES buffer + 0.4% BSA and activated with 10 μg/ml of αIgE for 5 min at 37°C. Cells were washed in 0.1% BSA in PBS and kept on ice, blocked with 3% BSA in PBS, then labeled with αFcεRI PE (eBioscience). Cells were analyzed on a CytoFLEX flow cytometer (Beckman Coulter). Statistical analysis was done by *t* tests comparing αIgE- or PrP(45-95)-treated samples to matching IgE alone (control or αPrP IgE) in GraphPad Prism 7.01 software. The presented histogram is from a single representative experiment.

Determination of phosphorylation of SYK and ERK by Western blot analysis

LAD2 cells were sensitized overnight with 25 ng/ml of commercial control IgE (HE1) or αPrP IgE. Cells were then resuspended in HEPES buffer without BSA and exposed to 10 μg/ml of αIgE for 5, 15, or 30 min or left unexposed (0-min time point). Cells were then lysed by adding 2× SDS lysis buffer (100 mM Tris, 4% SDS, 20% glycerol, 0.4% β-mercaptoethanol) + 2× cOmplete Protease Inhibitor Cocktail (Roche) + 2× Halt Phosphatase Inhibitor (Thermo Scientific), boiled, and analyzed by SDS-PAGE and Western blotting. Membranes were labeled with mouse αSYK (Abcam), rabbit αSYK (Phospho Y348; Abcam), mouse α-diphosphorylated ERK-1&2 (Sigma-Aldrich), and rabbit αERK1/2 (Cell Signaling Technology). Anti-rabbit 800 (LI-COR Biosciences) and α-mouse 680 (LI-COR Biosciences) were used as secondary Abs, and labeled membranes were analyzed by an Odyssey CLX Imaging System (LI-COR Biosciences). Gels are cropped to show bands at predicted sizes of markers, around the 70 kDa molecular mass marker for SYK and around the 38 kDa molecular mass marker for ERK.

ELISA analysis of chemokine and cytokine production

LAD2 cells were sensitized overnight with 25 ng/ml of commercial control IgE (HE1) or αPrP IgE. Cells were then washed and exposed to 10 μg/ml of αIgE or the indicated concentrations of PrP(45-95) for 20–24 h. Cells were isolated and analyzed by flow cytometry as indicated above. Supernatants were collected, and levels of CCL2, TNF, and IL-8 were assessed using the the corresponding human ELISA kits (R&D Systems) according to the manufacturer's protocol. CCL1 (I-309) was assessed with the human I-309 ELISA Kit (CCL1) (Abcam). For PGD2 release assays, LAD2 cells were sensitized with 25 ng/ml commercial control IgE (HE1) or αPrP IgE for 1–3 d. Cells were then exposed to 10 μg/ml of αIgE or 1 μg/ml of PrP(45-95). Supernatants were collected after 3 h and analyzed using PG D 2-MOX ELISA (Cayman Chemical Company). For samples exposed to varying concentrations of PrP(45-95), statistical analysis was done by comparing all samples with αPrP IgE only using one-way ANOVA with Dunnett's correction for multiple comparisons.

Analysis of protease release

LAD2 cells were sensitized with control IgE (HE1) or αPrP-IgE overnight, washed, and resuspended in HEPES buffer without BSA and activated by exposure to 10 μg/ml αIgE or 1 μg/ml of PrP(45-95) peptide for 30 min. Cells were then centrifuged, and supernatants were collected. Pellets were lysed in 1× SDS lysis buffer (described above) + 1× cOmplete Protease Inhibitor Cocktail (Roche). The equivalent of 5×10^5 lysed cells and an equivalent amount of supernatant were analyzed by Western blotting with mouse anti-tryptase (Neomarkers, Fremont, CA) or rabbit anti-cathepsin G (Cortex Biochem). All blots are cropped to show only bands at expected sizes of tryptase (around 30 kDa molecular mass marker) and cathepsin G (around 25 kDa molecular mass marker).

Statistical analysis

Statistical analysis was done using GraphPad Prism 7.01. For grouped data, multiple *t* tests with Holm-Sidak's correction was performed between treatments represented in the legends. Except where indicated otherwise in the *Materials and Methods* section, ungrouped graphs were compared with the untreated control using one-way ANOVA with multiple comparisons and Dunnett's correction.

Results

Effects of mast cell proteases on PrP

For an IgE-based immunotherapy to be effective, proteases from mast cell granules would need to degrade PrP. To assess if they could indeed do so, we exposed purified recombinant hamster PrP [recPrP(29-231)] to various mast cell enzymes and looked for changes in size and quantity via Coomassie staining (Fig. 1A). Notably, tryptase and, to a lesser extent, cathepsin G both reduced the total amount of protein and caused a smaller fragment to appear between 10 and 15 kDa. Neither tryptase nor cathepsin G had an effect on lysozyme (Fig. 1B), showing that digestion was not nonspecific. To further test whether mast cell proteases could digest PrP, we exposed recPrP(29-231) to conditioned supernatants from LAD2 cells degranulated with compound 48/80 (C48/80) (Fig. 1C). Here, mast cell supernatant caused several smaller

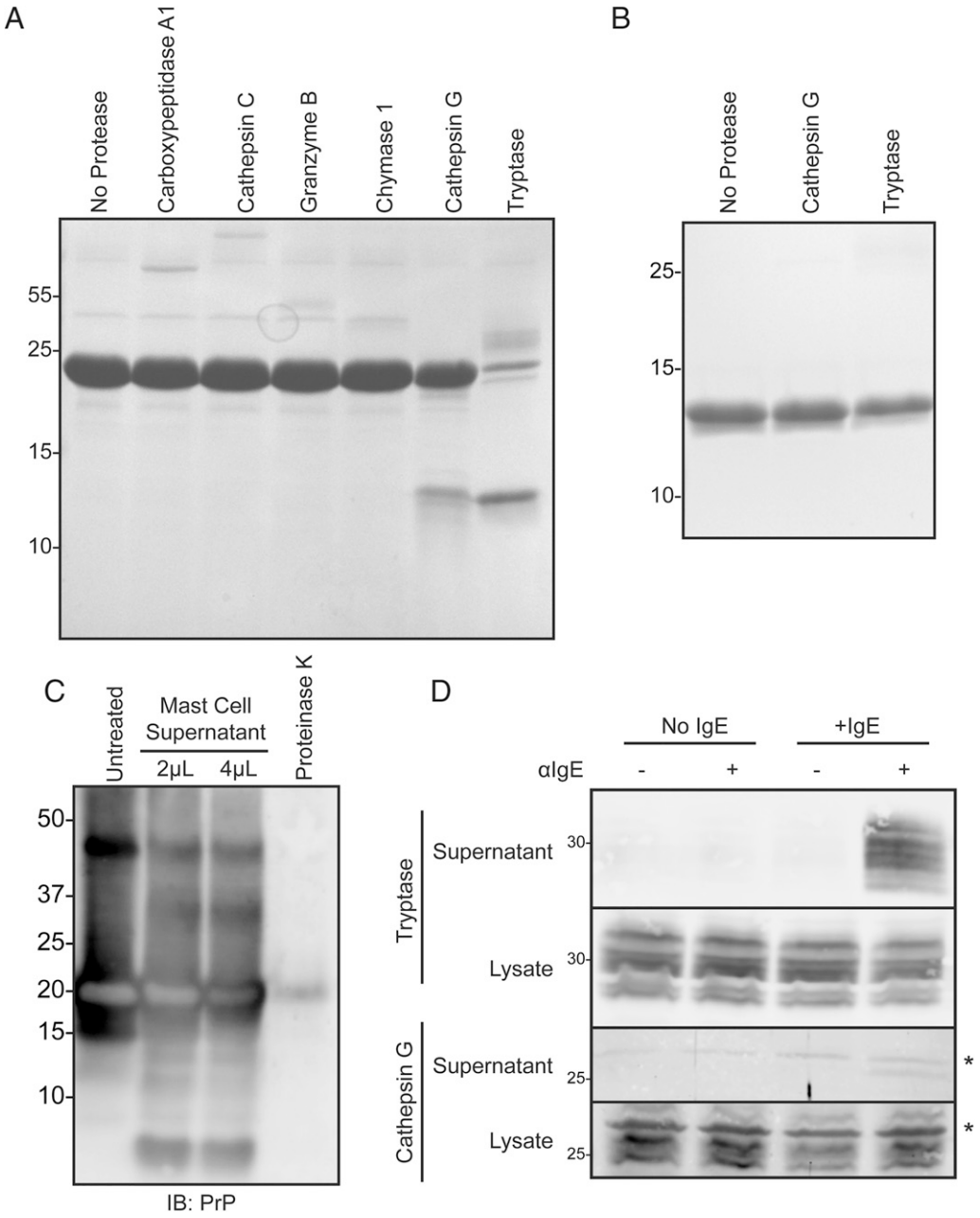

FIGURE 1. Effects of mast cell proteases on PrP. (**A**) A quantity of 15 μg of recPrP(29-231) or (**B**) lysozyme was exposed to commercial preparations of indicated proteases for 2.5 h at 37°C, then analyzed by SDS-PAGE and Coomassie staining. (**C**) A quantity of 10 μg of recPrP(29-231) was exposed to supernatant from degranulated mast cells or proteinase K for 1 h at 37°C. Digestion was then analyzed by Western blotting with an αPrP IgG. (**D**) LAD2 cells sensitized with commercial IgE were exposed to 10 μg/ml of αIgE to activate degranulation. Cells were then pelleted by centrifugation, supernatant was removed, and then the pellet was lysed. Lysate and supernatant were analyzed by Western blotting for tryptase and cathepsin G. *Nonspecific bands. Gel images were cropped to show relevant bands. Lysate and supernatant samples were run on the same gel and spliced for easier comparison.

PrP bands to appear, with a major band appearing below 10 kDa. Next, we determined whether tryptase and cathepsin G are released by LAD2 cells when activated through FcεRI and IgE crosslinking (Fig. 1D). Surprisingly, although a large amount of tryptase was released into the supernatant upon degranulation, the amount of cathepsin G was much more limited.

Construction and expression of αPrP IgE

To our knowledge, no PrP-specific IgE Ab has ever been reported. Because monoclonal IgE molecules are typically made from existing, previously characterized IgG molecules toward the intended target Ag (29), we engineered a chimeric αPrP IgE in which the V region was taken from a αPrP IgG reported previously. Two previously described humanized IgG mAbs, 13F10/3B5, that were successfully humanized and produced in a cell culture system were used as a template (27). These variable regions were chosen because their sequences were readily available and their binding characteristics had been previously described (30). DNA fragments corresponding to the variable regions of these Abs were synthesized and cloned into the pVITRO1-dV-IgE/k carrier (31) (Fig. 2A). Sequences of the variable regions are shown in Fig. 2B and 2C. The sequence to which the original αPrP IgG binds to PrP is shown in Fig. 3. All species of PrP used in this study are aligned to demonstrate that this region is highly conserved. The resulting plasmid was transiently transfected into mammalian suspension cells and produced recombinant mAbs that were isolated from the media by

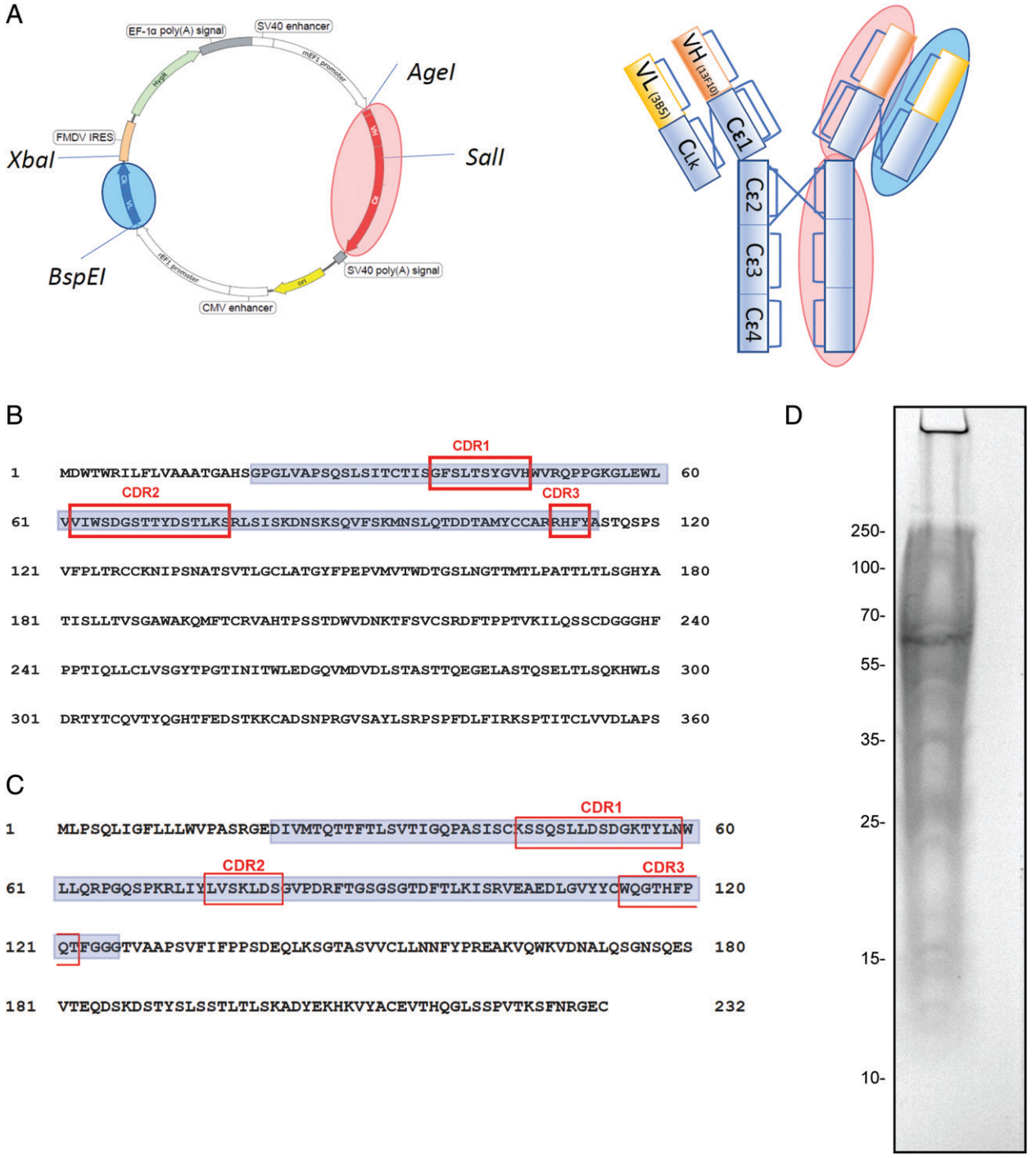

FIGURE 2. Construction, expression, and isolation of αPrP IgE. (**A**) Cloning strategy for αPrP IgE plasmid. Amino acid sequences of the H (**B**) and L (**C**) chains of PrP-IgE. Blue indicates L chain, and red indicates CD regions. (**D**) αPrP IgE was subjected to denaturing SDS-PAGE and analyzed by Coomassie blue staining. Gel image was cropped to show relevant lane only.

CHT chromatography. When analyzing Ab stock by SDS-PAGE and Coomassie staining (Fig. 2D), staining was diffuse rather than concentrated in two small bands at the expected sizes of the H and L chains, at 70 kDa and 25 kDa, respectively. This may be due to heterogeneity of post-translational modifications and incomplete oxidation of disulfide bonds within the Ab stock.

Testing activation of mast cells by αPrP IgE

To ensure that the IgE C region was correctly folded, its ability to bind and activate mast cells was tested. First, LAD2 cells were exposed to the αPrP IgE or a commercial IgE overnight. Binding was then assessed by labeling with an allophycocyanin-labeled αIgE Ab and measuring fluorescence via flow cytometry (Fig. 4A). Notably, both IgEs caused a significant increase in fluorescence relative to cells not exposed to IgE. The control IgE showed a greater shift, but this may be due to the increased purity of the commercial IgE stock. Because mast cells are known to express PrP (32), we sought to ensure that the αPrP IgE was binding to mast cells through IgE receptors and not through binding PrP itself. To do this, IgE was preincubated with omalizumab, an Ab directed toward IgE that inhibits binding of IgE to its receptors (33). This αIgE was able to successfully inhibit binding of both αPrP IgE and the control IgE to LAD2

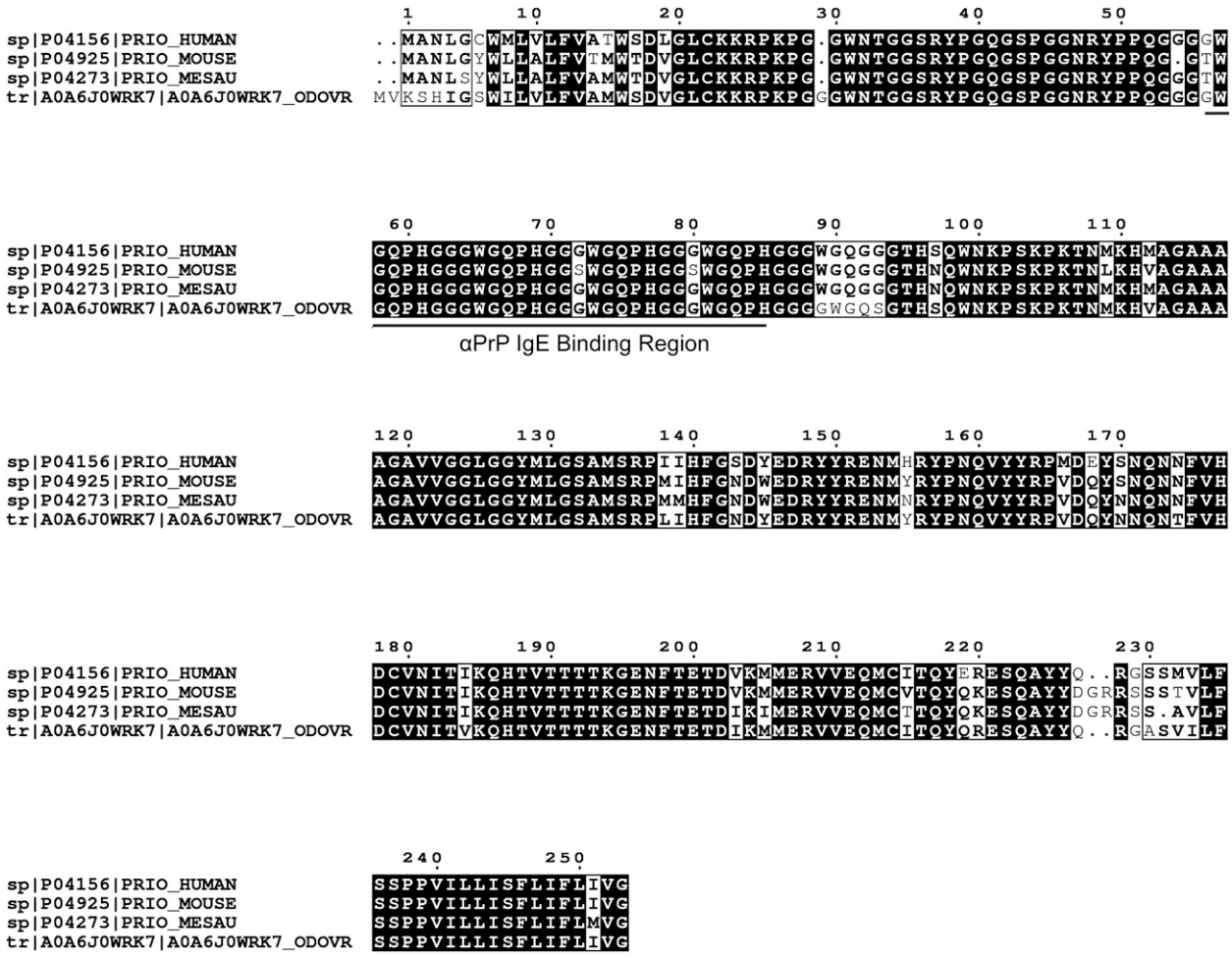

FIGURE 3. PrP amino acid sequences from human, mouse, hamster, and deer were aligned using Clustal Ω (25) and visualized using ESPript 3.0 (69). The region containing repetitive epitopes bound by the Abs used to construct αPrP IgE is indicated by a gray line.

cells (Fig. 4B), showing that the interaction is almost entirely through the IgE receptor and not through binding of the Ab to its Ag.

Next, to ensure that the αPrP Ab could activate mast cells, degranulation after activation was measured (Fig. 4C). LAD2 cells were preloaded with a control IgE, αPrP IgE, or no IgE overnight and exposed to an αIgE IgG Ab. This second Ab is expected to cluster IgE molecules, activating the IgE receptors they are attached to. The αPrP IgE was able to induce degranulation in LAD2 cells at 25 ng/ml and 5 ng/ml concentrations, though not at the lowest concentration of 1 ng/ml. The control Ab was able to activate the receptor to a greater extent at all three concentrations, possibly due to the higher purity of the commercial preparation. Activation of LAD2 through αPrP IgE and αIgE also induced a decrease in surface expression of the IgE receptor, FcεRI (Fig. 4D). This is a further indication that the αPrP IgE is functioning through FcεRI, because this receptor is known to be endocytosed after activation (34).

Other downstream pathways are activated by αPrP IgE

Further evidence that αPrP IgE can activate LAD2 cells through the FcεRI receptor was shown by its ability to induce phosphorylation of the downstream signaling molecules SYK and ERK (Fig. 5A). SYK is a tyrosine kinase that binds to phosphotyrosines on the cytoplasmic side of the FcεRI, whereas ERK is phosphorylated later during a MAPK cascade (35). Phosphorylation of SYK and ERK peaked at 5 min before becoming undetectable at 15 and 30 min in SYK and ERK, respectively. Notably, αPrP IgE showed weaker activation than control IgE, possibly explaining the lower levels of degranulation seen for this Ab. The αPrP IgE was also able to cause release of tryptase into the supernatant (Fig. 5B). As an alternative means to measure activation of LAD2 cells through the FcεRI receptor, we next sought to determine whether αPrP IgE could induce the release of signaling molecules. Because the chemokine CCL2, also known as MCP-1, has previously been found to be released from mast cells after activation (22), we next determined whether αPrP IgE could induce the release of CCL2 from LAD2 cells. Both control and αPrP IgE failed to increase CCL2 release after activation (Fig. 5C). Similar results were seen for release of another chemokine, CCL1, and PGD2 (Fig. 5C and D). Several additional cytokines were tested but found not to be released from LAD2 cells when activated via commercial IgE or αPrP IgE cross-linking (data not shown). Ultimately, release of cytokines from LAD2 did not prove to be a suitable method by which to detect activation through the FcεRI receptor when activated with IgE/anti-IgE.

Binding of αPrP IgE to its Ag

To determine whether αPrP IgE could bind PrP protein, we used Western blot analysis to detect binding to various sources of PrP (Fig. 6A). Here, the αPrP IgE was able to bind to large amounts (10 μg) of recombinant mouse PrP(23-231) but failed to bind lower amounts of endogenous cellular PrP^C from 10-μg brain homogenates of various species. Further attempts to assess binding ability by ELISA or surface plasmon resonance (data not shown) failed to show binding to lower amounts of PrP, suggesting binding affinity is weak. Given the sensitivity of mast cells to IgE-induced activation, we next

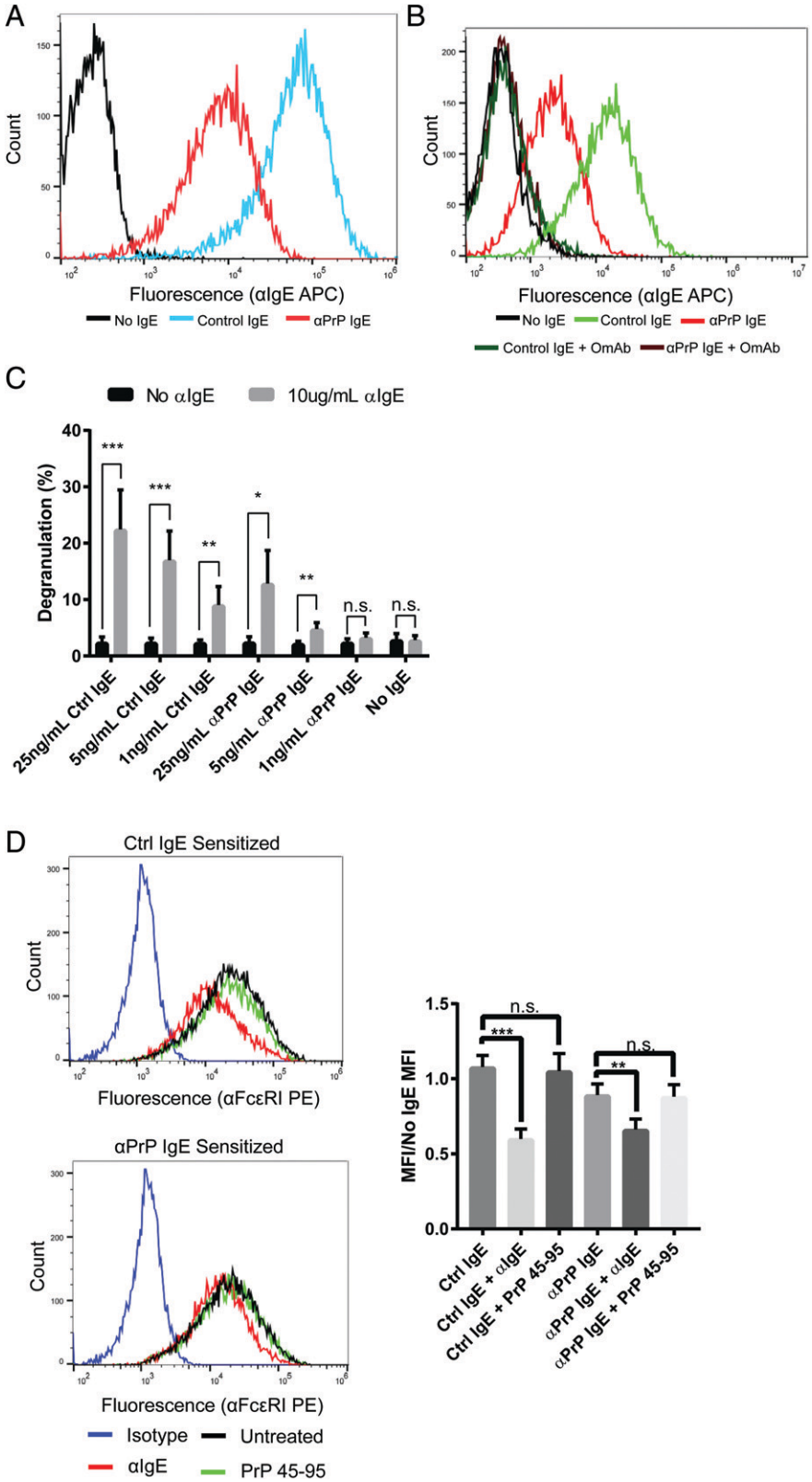

FIGURE 4. Testing the ability of the αPrP IgE to activate mast cells. (**A**) LAD2 cells were incubated with no IgE, αPrP IgE, or a control IgE overnight. Cells were then stained with αIgE IgG allophycocyanin (APC) and analyzed by flow cytometry. Histograms of allophycocyanin fluorescence (IgE staining) are shown for each incubation condition. (**B**) The αPrP IgE or a control IgE (Ctrl IgE) were preincubated with or without the Ab omalizumab (OmAb), which blocks binding of IgE to Fc receptors. LAD2 cells were then exposed to these Abs for 1 h before staining with an allophycocyanin-linked αIgE Ab, and fluorescence was determined by flow cytometry. (**C**) LAD2 cells were incubated with no IgE, αPrP IgE, or a control IgE overnight. Bound IgE was then cross-linked with αIgE IgG, and degranulation was measured by a β-hexosaminidase release assay ($n = 5$). (**D**) LAD2 cells were sensitized with the indicated IgE or no IgE. Activation was induced with 10 μg/ml αIgE IgG or 1 μg/ml PrP(45-95) for 5 min, and FcεRI surface expression was determined by FACS ($n = 4$). All samples are from a single representative experiment. A single isotype control sample is shown twice, once in each histogram. $*p < 0.05$, $**p < 0.01$, $***p < 0.001$.

tested the ability of αPrP IgE-sensitized LAD2 cells to activate in response to exposure to a PrP peptide containing the epitope bound by αPrP IgE (aa 45 to 95) (Fig. 6B–6D). Here, exposure to peptide did not result in a significant change in CCL2, CCL1, or PGD2 release compared with nonactivated cells. Notably, αPrP IgE-sensitized LAD2 cells exposed to PrP peptide also did not release more tryptase into the media than nonactivated cells (Fig. 5B). Although the PrP peptide should contain multiple epitopes for αPrP IgE, these epitopes are clustered together, so it is possible that multiple Abs are unable to bind this peptide at once, which would prevent crosslinking necessary to activate the IgE receptor. We also tested the ability of PrP fibrils composed of many PrP monomers to activate αPrP-sensitized LAD2 (Fig. 6E). Here, too, fibrils showed no effect, suggesting that the epitope may be less accessible in the fibril form or that the αPrP IgE likely lacks sufficient binding to its Ag to induce a response in LAD2 cells.

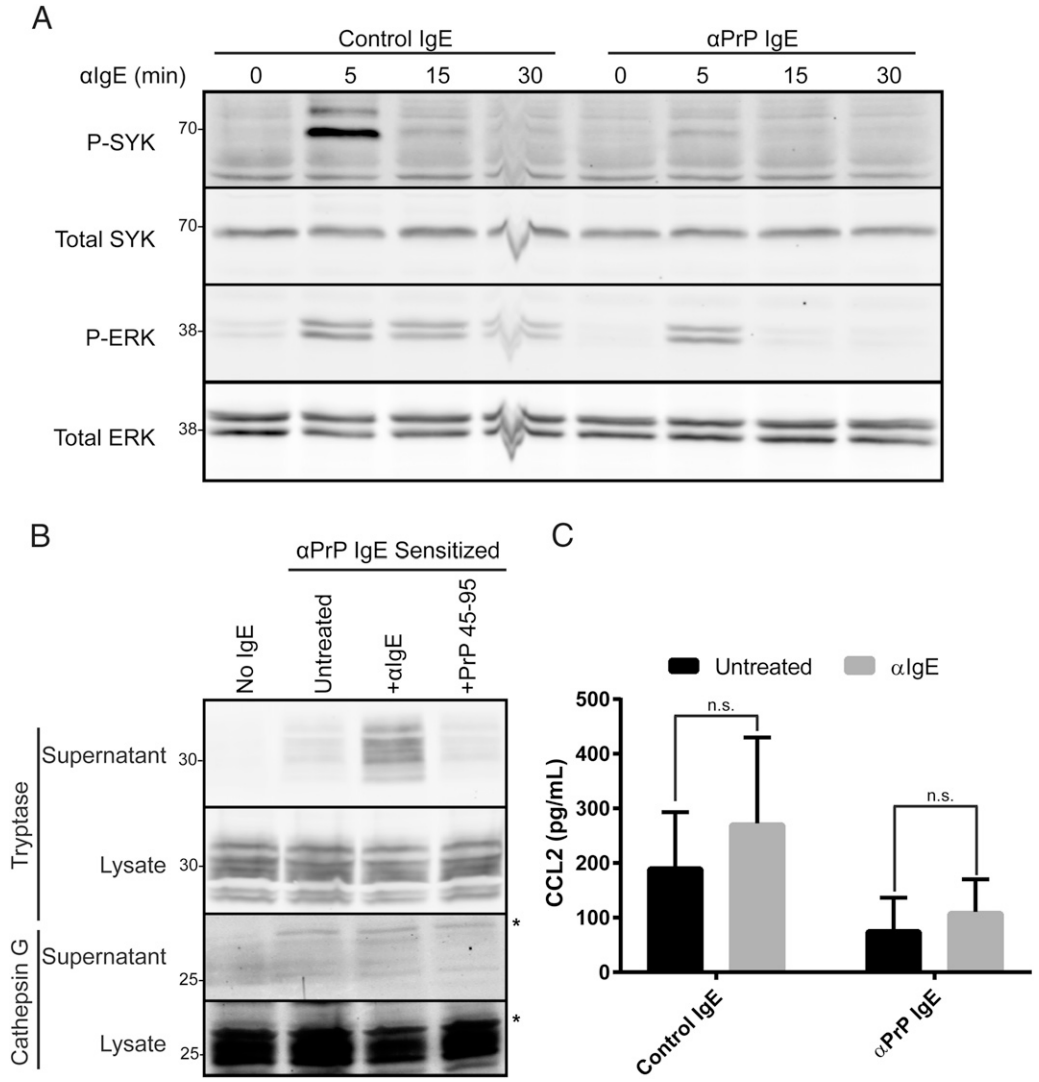

FIGURE 5. The αPrP IgE can activate other responses downstream of FcεRI. (**A**) LAD2 cells were sensitized with αPrP IgE or a control IgE overnight. Cells were then activated by exposure to αIgE for 5, 15, or 30 min, then lysed. Phosphorylation of SYK (Y348) or ERK was determined by Western blot analysis. (**B**) LAD2 cells were sensitized with αPrP-IgE overnight and activated with αIgE or a peptide representing residues 45-95 of human PrP for 30 min. Cells were centrifuged, and supernatant was collected while the pellet was lysed. Both lysate and supernatants were analyzed by Western blotting with the indicated Abs. *Nonspecific bands. (**C**) LAD2 cells were sensitized with control IgE (Ctrl IgE) or αPrP IgE, then activated by αIgE for 20 h. Supernatants were then collected and analyzed for CCL2 release via ELISA ($n = 3$). No statistically significant differences were found between untreated and αIgE-treated cells. Gel images were cropped to display only relevant bands. Lysate and supernatant samples were run on the same gel and spliced for easier comparison.

Changes to cell surface markers after exposure to Ag

To further test whether αPrP IgE could induce a response in LAD2 cells when exposed to its Ag, the ability of the PrP peptide to activate αPrP IgE and induce changes to cell surface receptors (Fig. 7) was evaluated. Here, PrP peptide induced increases in FcεRI and CD203c expression similar to those of control IgE + αIgE as compared with untreated cells (Fig. 7A, 7B). CD203c is a specific marker for mast cells and basophils that is upregulated after FcεRI activation (36). Likewise, both control IgE + αIgE and αPrP IgE + peptide induced decreases in CD29, or integrin β1, cell surface expression, whereas only control IgE + αIgE had an effect on C3aR.

Discussion

Prions are transmissible pathogenic agents responsible for fatal diseases such as bovine spongiform encephalopathy, chronic wasting disease, and Creutzfeldt-Jakob disease. No effective therapies for prion diseases exist. The key event in prion disease is the conversion of cellular prion protein (PrP^C) into the infectious form, PrP^{Sc} (37). Small-molecule drugs with antiprion activity in vitro have been identified (23, 38) but have proved ineffective or toxic in vivo (39–41). Immunotherapy overcomes these challenges because injection of Ag-specific Ig can effectively neutralize infection without damaging healthy tissues. Increasing the strength and breadth of PrP-specific cellular immune responses may also provide a clinical benefit: Immune tissues appear to be involved in peripherally acquired prion disease (42–44), the immune system may facilitate prion entry via the gut (45), and PrP^C may have a physiological role in some immune cells (46, 47). Many Abs against PrP epitopes have been made on the basis of IgG (48–50), but they are largely ineffective or only slightly slow disease progression in vivo (51, 52). This failure may be due to several factors. Existing Abs have mainly aimed to bind PrP^C and interfere with its misfolding rather than to engage the cellular immune response. In contrast, it is becoming increasingly clear from work on other diseases such as cancer that to develop a successful immunotherapy, the entire repertoire of the immune response (humoral as

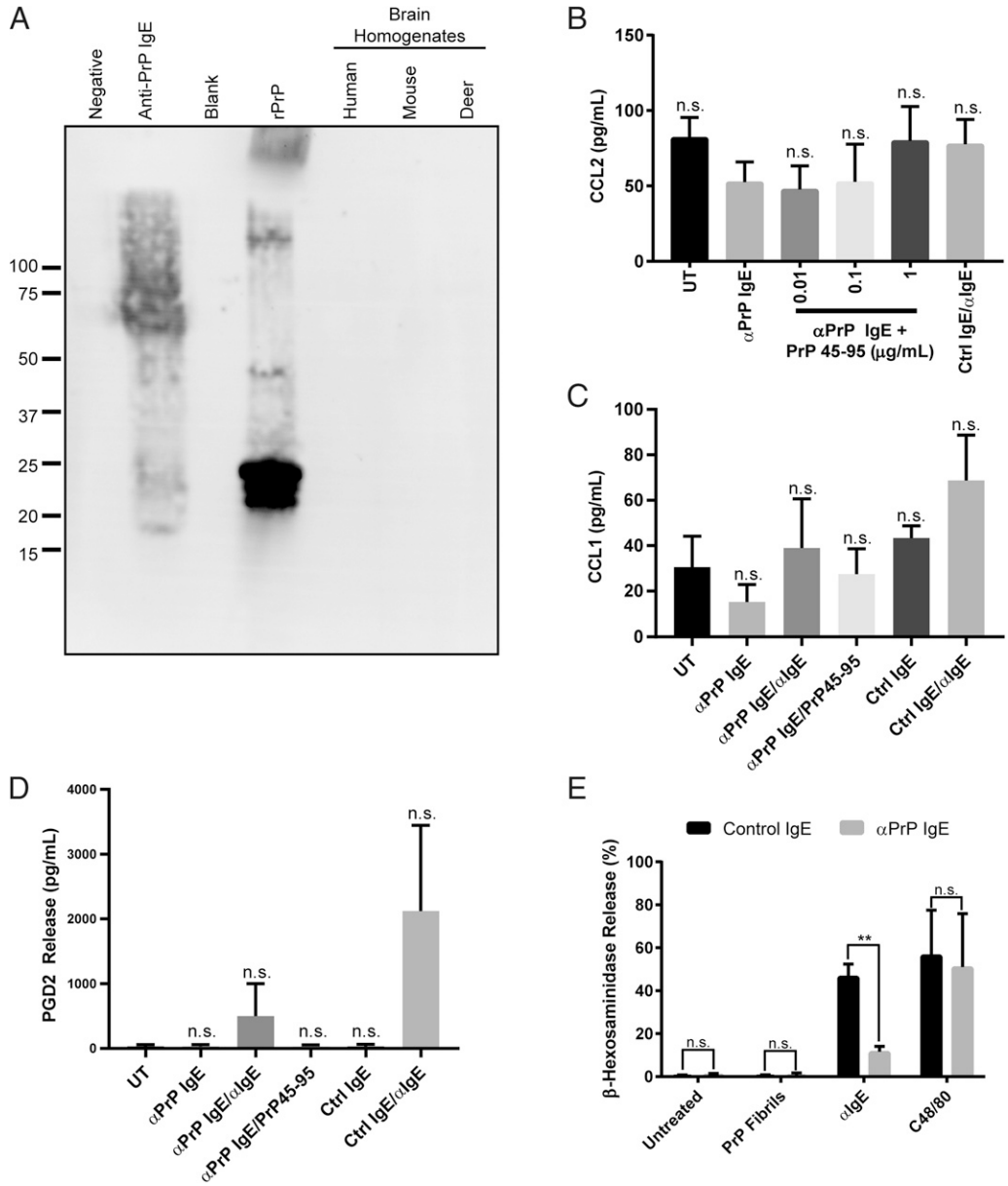

FIGURE 6. Testing the ability of the αPrP IgE to bind its Ag. (**A**) Anti-PrP IgE was used as a primary Ab in a Western blot to determine binding to several PrP-containing samples. Samples used include a PrP-free lysate (Negative); the αPrP IgE itself; buffer only (Blank); a recombinant PrP derived from bacteria (rPrP); and brain homogenates from human, mouse, and deer. Gel image was cropped to show indicated lanes. (**B**) LAD2 cells were left untreated (UT) or sensitized with αPrP IgE or control IgE (Ctrl IgE), then activated with αIgE or a peptide representing aa 45 to 95 of human PrP [PrP(45-90)] for 24 h. Supernatants were then collected, and CCL2 levels were assessed by ELISA ($n = 3$). (**C**) LAD2 cells were treated as in (B), and levels of CCL1 were assessed by ELISA ($n = 3$). (**D**) LAD2 cells were sensitized as in (B) and activated with αIgE or PrP(45-95) for 3 h. Supernatants were collected, and PGD2 levels were assessed by ELISA ($n = 3$). (**E**) LAD2 cells were sensitized with αPrP IgE or a control IgE overnight. Sensitized cells were then activated by αIgE, PrP fibrils, or C48/80 for 1 h, and degranulation was measured by a β-hexosaminidase release assay ($n = 3$). $^{**}p < 0.01$.

well as cellular) must be mobilized (53). Moreover, the Abs have trouble crossing the blood–brain barrier and face three critical immunological hurdles (54): PrP^C is endogenous, hence immunotherapy must break immune-tolerance; IgG itself may cause neurotoxicity by activating inflammation (55); and large doses must be supplied to the infection site to reduce PrP content, only postponing symptom onset (56, 57). The poor response to IgGs may arise from poor transport of IgG in tissues and across the blood–brain barrier (12) (IgG is mainly a serum Ab), and/or the high endogenous blood levels of IgG (requiring high doses of therapeutic IgG to overcome competition for Fc receptor binding, a problem common in IgG-based immunotherapy [58]). Similarly disappointing results from initially promising Abs have been found for IgG-based immunotherapeutic approaches for other misfolding-related neurodegenerative diseases such as Alzheimer's disease, Parkinson's disease, and amyotrophic lateral sclerosis (59–62). Existing immunotherapy strategy thus has significant drawbacks, and a new approach to αPrP Ab design is required—one that overcomes at least some of these challenges.

Here, we present the construction of an IgE class Ab directed toward the prion protein. Although relatively understudied as therapeutics, IgE Abs have recently found use as anticancer agents (29). Initially, an analogy was drawn between targeting solid tumors and one of IgE's traditional roles in expunging parasites (29). This analogy may be extended to PrP aggregates, which are also large structures that need to be broken down. Notably, a large portion of mast cell granule protein is proteases (2), which could potentially degrade PrP aggregates,

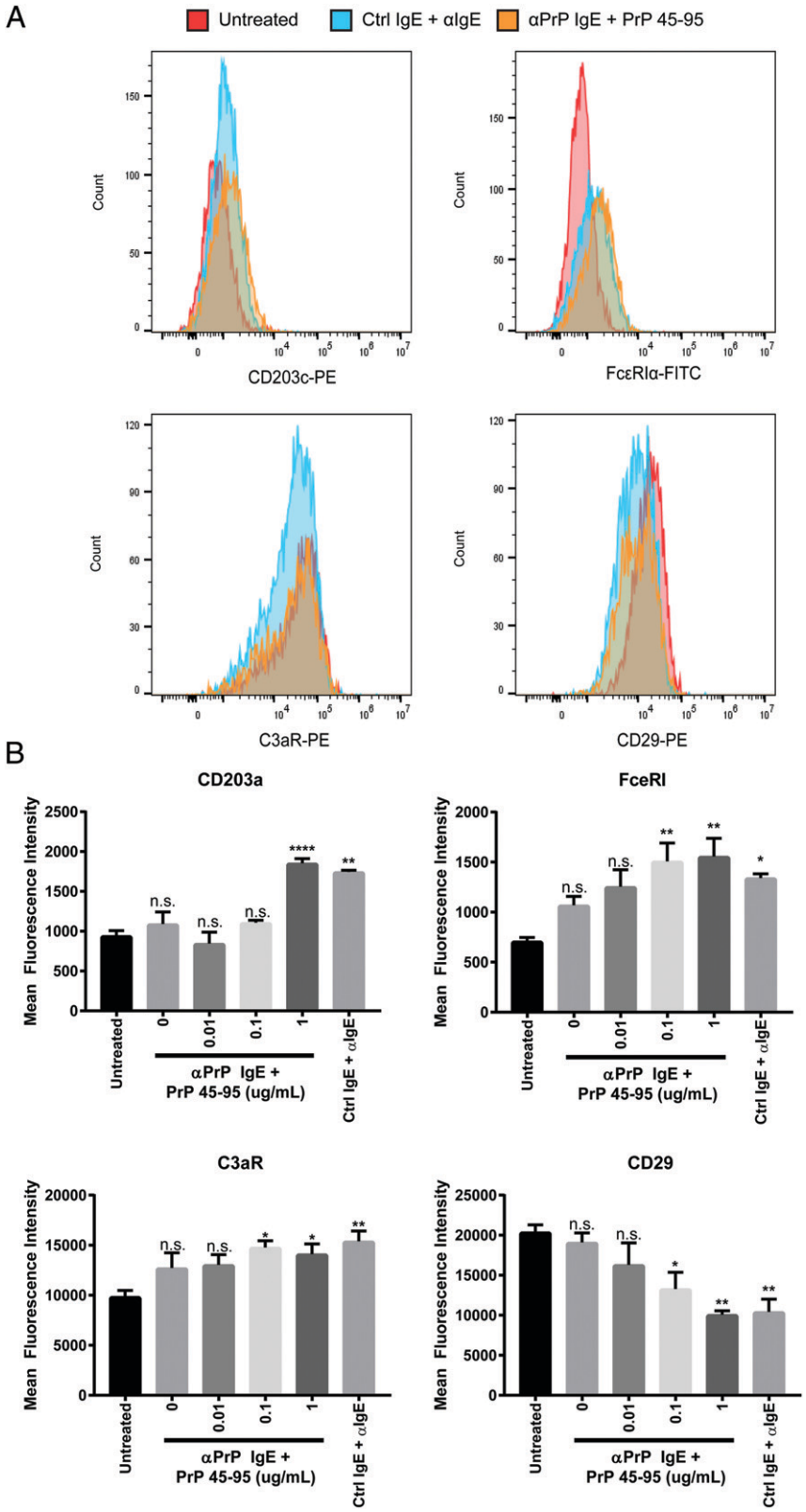

FIGURE 7. Changes to surface expression of biomarkers after αPrP IgE-sensitized cells are exposed to PrP(45-95). (**A**) LAD2 cells were sensitized with αPrP IgE or control IgE overnight, then exposed to anti-IgE or indicated concentrations of PrP(45-95) for 24 h. Cells were labeled with Abs to CD203c, FcεRI, C3aR, and CD29 and analyzed by flow cytometry ($n = 3$). (**B**) Average mean fluorescence intensity of given markers from (A). $*p < 0.05$, $**p < 0.01$, $****p < 0.0001$.

particularly the earliest formed oligomers, which are more protease sensitive (63). Alternatively, mast cells could recruit other cells of the immune system to clear PrP aggregates and destroy infected cells. Because mast cells are usually present at the periphery, including the gut mucosa, IgE could also function prophylactically, allowing early recognition and destruction of ingested PrP^{Sc}.

Given their therapeutic potential in prion disease, we initially tested whether mast cell proteases could target PrP. Using isolated proteases in an in vitro assay, we found that tryptase and, to a lesser extent, cathepsin G were able to decrease the level of recombinant PrP and lead to the formation of a smaller fragment between 10 and 15 kDa. When rPrP was exposed to supernatant from degranulated

LAD2 cells, several smaller fragments appeared, although the effect on overall protein levels was less apparent. This effect was likely mediated mostly by tryptase, because it had a larger effect in in vitro experiments and was released in significant amounts after activation, in contrast to cathepsin G. The precise amino acid sequence where mast cell proteases cleave PrP has yet to be determined, but a previous study by Haddon et al. (32) revealed that PrP was released from the surface of degranulated mast cells. This suggests that protease cleavage may occur somewhere in the C-terminus, separating the bulk of PrP from its GPI anchor (64). Given that PrP^{Sc} is only able to cause cell death in neurons expressing PrP^{C} (65), effector cell proteases could reduce the amount of PrP^{C} on the surface of neurons near PrP^{Sc} plaques, thereby reducing neurodegeneration. Notably, increasing protease-induced shedding of PrP from the surface of neurons reduces the toxicity of both PrP^{Sc} and amyloid-β oligomers (66, 67), further supporting the idea of targeting PrP^{C} with proteases. Reduction in PrP^{C} levels could also slow down PrP^{Sc} conversion and propagation.

The αPrP Ab we generated proved to be effective in binding mast cells, suggesting that the Fc portion of the molecule is intact and can bind the IgE receptor. This was further shown by the ability of omalizumab, an αIgE Ab capable of preventing IgE binding to Fc receptors, to block αPrP IgE binding. The αPrP IgE was also shown to be functionally active, because IgE-loaded LAD2 mast cells degranulated when exposed to αIgE and induced the phosphorylation of downstream kinases and release of proteases. Ultimately, these experiments show that the LAD2 mast cell line is an effective tool for characterizing chimeric IgE molecules. Notably, LAD2 cells show similar levels of high-affinity IgE receptor and histamine release after IgE-induced degranulation compared with human skin mast cells (68). In contrast, the other common human mast cell line, HMC-1, showed little if any IgE-induced histamine release and much lower levels of IgE receptor (68). Although LAD2 cells express lower levels of some proteases than human skin mast cells (68), they do express enough of some proteases to have an effect on PrP in vitro. For these reasons, LAD2 cells will likely prove a good model system for initial functional characterization of synthetic IgEs before transitioning to more expensive and difficult to obtain human mast cells from human tissues. Some limitations do exist, though, and LAD2 cells were not found to release significant amounts of CCL-2 and other chemokines after degranulation compared with nonactivated cells.

Although the αPrP IgE showed some binding to its Ag, overall binding was not sufficient to induce degranulation of LAD2 cells after exposure to its Ag. Some changes in gene expression and surface biomarker expression were evident, though. This suggests that the αPrP IgE has low affinity for the PrP Ags tested herein. Certainly, an important recent study by Suzuki et al. has shown that IgEs with low affinity for their Ag shifts signals from the adapter LAT1 (linker of activation of T cells 1) to the related adapter LAT2 such that degranulation is dampened but chemokine production is enhanced (17). This suggests that low-affinity IgE, such as the one that we have engineered, may actually be beneficial in altering immune cell recruitment at the site of inflammation without initiating an anaphylactic response through degranulation. Further design optimization may still need to be done to improve Ag recognition and affinity. The study from which the original αPrP IgG sequences were derived (27) does not offer binding data, suggesting a change in variable regions may be necessary. Nevertheless, the present work demonstrates the feasibility of eliciting mast cell enzymes to degrade PrP and sets up an efficient system using the LAD2 cell line for characterizing the function of synthetic IgE molecules. Future work will therefore use our LAD2 model to test additional αPrP Abs and further investigate the ability of mast cells to clear PrP^{Sc} infection.

Acknowledgments

We thank Ashley Wagner and Narcy Arizmendi for their technical assistance and Leonardo Cortez for production of PrP fibrils.

Disclosures

The authors have no financial conflicts of interest.

References

1. Fitzsimmons, C. M., F. H. Falcone, and D. W. Dunne. 2014. Helminth allergens, parasite-specific IgE, and its protective role in human immunity. *Front. Immunol.* 5: 61.
2. Stone, K. D., C. Prussin, and D. D. Metcalfe. 2010. IgE, mast cells, basophils, and eosinophils. *J. Allergy Clin. Immunol.* 125(2 Suppl 2): S73–S80.
3. Moon, T. C., A. D. Befus, and M. Kulka. 2014. Mast cell mediators: their differential release and the secretory pathways involved. *Front. Immunol.* 5: 569.
4. Wernersson, S., and G. Pejler. 2014. Mast cell secretory granules: armed for battle. *Nat. Rev. Immunol.* 14: 478–494.
5. Perez, E. E., J. S. Orange, F. Bonilla, J. Chinen, I. K. Chinn, M. Dorsey, Y. El-Gamal, T. O. Harville, E. Hossny, B. Mazer, et al. 2017. Update on the use of immunoglobulin in human disease: A review of evidence. *J. Allergy Clin. Immunol.* 139(3S): S1–S46.
6. Sutton, B. J., and A. M. Davies. 2015. Structure and dynamics of IgE-receptor interactions: FcεRI and CD23/FcεRII. *Immunol. Rev.* 268: 222–235.
7. Shelburne, C. P., and S. N. Abraham. 2011. The mast cell in innate and adaptive immunity. *Adv. Exp. Med. Biol.* 716: 162–185.
8. Negrão-Corrêa, D., L. S. Adams, and R. G. Bell. 1996. Intestinal transport and catabolism of IgE: a major blood-independent pathway of IgE dissemination during a *Trichinella spiralis* infection of rats. *J. Immunol.* 157: 4037–4044.
9. Teo, P. Z., P. J. Utz, and J. A. Mollick. 2012. Using the allergic immune system to target cancer: activity of IgE antibodies specific for human CD20 and MUC1. *Cancer Immunol. Immunother.* 61: 2295–2309.
10. Josephs, D. H., J. F. Spicer, P. Karagiannis, H. J. Gould, and S. N. Karagiannis. 2014. IgE immunotherapy: a novel concept with promise for the treatment of cancer. *MAbs* 6: 54–72.
11. Leoh, L. S., T. R. Daniels-Wells, and M. L. Penichet. 2015. IgE immunotherapy against cancer. *Curr. Top. Microbiol. Immunol.* 388: 109–149.
12. Vidarsson, G., G. Dekkers, and T. Rispens. 2014. IgG subclasses and allotypes: from structure to effector functions. *Front. Immunol.* 5: 520.
13. Muldoon, L. L., C. Soussain, K. Jahnke, C. Johanson, T. Siegal, Q. R. Smith, W. A. Hall, K. Hynynen, P. D. Senter, D. M. Peereboom, and E. A. Neuwelt. 2007. Chemotherapy delivery issues in central nervous system malignancy: a reality check. *J. Clin. Oncol.* 25: 2295–2305.
14. Daniels-Wells, T. R., G. Helguera, R. K. Leuchter, R. Quintero, M. Kozman, J. A. Rodríguez, E. Ortiz-Sánchez, O. Martínez-Maza, B. C. Schultes, C. F. Nicodemus, and M. L. Penichet. 2013. A novel IgE antibody targeting the prostate-specific antigen as a potential prostate cancer therapy. *BMC Cancer* 13: 195.
15. Reber, L. L., J. D. Hernandez, and S. J. Galli. 2017. The pathophysiology of anaphylaxis. *J. Allergy Clin. Immunol.* 140: 335–348.
16. Spicer, J., B. Basu, A. Montes, U. Banerji, R. Kristeleit, G. J. Veal, C. Corrigan, S. Till, G. Nintos, T. Brier, et al. 2020. Abstract CT141: Phase 1 trial of MOv18, a first-in-class IgE antibody therapy for cancer. *Cancer Res.* 80(16_Suppl): CT141.
17. Suzuki, R., S. Leach, W. Liu, E. Ralston, J. Scheffel, W. Zhang, C. A. Lowell, and J. Rivera. 2014. Molecular editing of cellular responses by the high-affinity receptor for IgE. *Science* 343: 1021–1025.
18. Chang, X., L. Zha, A. Wallimann, M. O. Mohsen, P. Krenger, X. Liu, M. Vogel, and M. F. Bachmann. 2021. Low-affinity but high-avidity interactions may offer an explanation for IgE-mediated allergen cross-reactivity. *Allergy* 76: 2565–2574.
19. Jucker, M., and L. C. Walker. 2013. Self-propagation of pathogenic protein aggregates in neurodegenerative diseases. *Nature* 501: 45–51.
20. Greenlee, J. J., and M. H. Greenlee. 2015. The transmissible spongiform encephalopathies of livestock. *ILAR J.* 56: 7–25.
21. Sikorska, B., and P. P. Liberski. 2012. Human prion diseases: from Kuru to variant Creutzfeldt-Jakob disease. *Subcell. Biochem.* 65: 457–496.
22. Fang, X., H. Hu, J. Xie, H. Zhu, D. Zhang, W. Mo, R. Zhang, and M. Yu. 2012. An involvement of neurokinin-1 receptor in FcεRI-mediated RBL-2H3 mast cell activation. *Inflamm. Res.* 61: 1257–1263.
23. Sandhu, J. K., and M. Kulka. 2021. Decoding mast cell-microglia communication in neurodegenerative diseases. *Int. J. Mol. Sci.* 22: 1093.
24. Bradford, B. M., and N. A. Mabbott. 2012. Prion disease and the innate immune system. *Viruses* 4: 3389–3419.
25. Madeira, F., M. Pearce, A. R. N. Tivey, P. Basutkar, J. Lee, O. Edbali, N. Madhusoodanan, A. Kolesnikov, and R. Lopez. 2022. Search and sequence analysis tools services from EMBL-EBI in 2022. *Nucleic Acids Res.* 50: W276–W279.
26. Cortez, L. M., J. Kumar, L. Renault, H. S. Young, and V. L. Sim. 2013. Mouse prion protein polymorphism Phe-108/Val-189 affects the kinetics of fibril

formation and the response to seeding: evidence for a two-step nucleation polymerization mechanism. *J. Biol. Chem.* 288: 4772–4781.
27. Mueller, D. A., L. Heinig, S. Ramljak, A. Krueger, R. Schulte, A. Wrede, and A. W. Stuke. 2010. Conditional expression of full-length humanized anti-prion protein antibodies in Chinese hamster ovary cells. *Hybridoma (Larchmt.)* 29: 463–472.
28. Kuehn, H. S., M. Radinger, and A. M. Gilfillan. 2010. Measuring mast cell mediator release. *Curr. Protoc. Immunol.* Chapter 7: Unit7.38.
29. Sutton, B. J., A. M. Davies, H. J. Bax, and S. N. Karagiannis. 2019. IgE antibodies: from structure to function and clinical translation. *Antibodies (Basel)* 8: 19.
30. Krasemann, S., M. H. Groschup, S. Harmeyer, G. Hunsmann, and W. Bodemer. 1996. Generation of monoclonal antibodies against human prion proteins in PrP0/0 mice. *Mol. Med.* 2: 725–734.
31. Dodev, T. S., P. Karagiannis, A. E. Gilbert, D. H. Josephs, H. Bowen, L. K. James, H. J. Bax, R. Beavil, M. O. Pang, H. J. Gould, et al. 2014. A tool kit for rapid cloning and expression of recombinant antibodies. *Sci. Rep.* 4: 5885.
32. Haddon, D. J., M. R. Hughes, F. Antignano, D. Westaway, N. R. Cashman, and K. M. McNagny. 2009. Prion protein expression and release by mast cells after activation. *J. Infect. Dis.* 200: 827–831.
33. Schulman, E. S. 2001. Development of a monoclonal anti-immunoglobulin E antibody (omalizumab) for the treatment of allergic respiratory disorders. *Am. J. Respir. Crit. Care Med.* 164(Suppl 1): S6–S11.
34. Fattakhova, G., M. Masilamani, F. Borrego, A. M. Gilfillan, D. D. Metcalfe, and J. E. Coligan. 2006. The high-affinity immunoglobulin-E receptor (FcεRI) is endocytosed by an AP-2/clathrin-independent, dynamin-dependent mechanism. *Traffic* 7: 673–685.
35. Kopeć, A., B. Panaszek, and A. M. Fal. 2006. Intracellular signaling pathways in IgE-dependent mast cell activation. *Arch. Immunol. Ther. Exp. (Warsz.)* 54: 393–401.
36. Bühring, H. J., P. J. Simmons, M. Pudney, R. Müller, D. Jarrossay, A. van Agthoven, M. Willheim, W. Brugger, P. Valent, and L. Kanz. 1999. The monoclonal antibody 97A6 defines a novel surface antigen expressed on human basophils and their multipotent and unipotent progenitors. *Blood* 94: 2343–2356.
37. Caughey, B., and G. J. Raymond. 1991. The scrapie-associated form of PrP is made from a cell surface precursor that is both protease- and phospholipase-sensitive. *J. Biol. Chem.* 266: 18217–18223.
38. Kamatari, Y. O., Y. Hayano, K. Yamaguchi, J. Hosokawa-Muto, and K. Kuwata. 2013. Characterizing antiprion compounds based on their binding properties to prion proteins: implications as medical chaperones. *Protein Sci.* 22: 22–34.
39. Doh-ura, K. 2004. Prion diseases: disease diversity and therapeutics. [Article in Japanese.] *Rinsho Shinkeigaku* 44: 855–856.
40. Priola, S. A., A. Raines, and W. S. Caughey. 2000. Porphyrin and phthalocyanine antiscrapie compounds. *Science* 287: 1503–1506.
41. Rudyk, H., S. Vasiljevic, R. M. Hennion, C. R. Birkett, J. Hope, and I. H. Gilbert. 2000. Screening Congo Red and its analogues for their ability to prevent the formation of PrP-res in scrapie-infected cells. *J. Gen. Virol.* 81: 1155–1164.
42. Kimberlin, R. H., and C. A. Walker. 1989. The role of the spleen in the neuroinvasion of scrapie in mice. *Virus Res.* 12: 201–211.
43. Hadlow, W. J., R. E. Race, and R. C. Kennedy. 1987. Temporal distribution of transmissible mink encephalopathy virus in mink inoculated subcutaneously. *J. Virol.* 61: 3235–3240.
44. Hilton, D. A., E. Fathers, P. Edwards, J. W. Ironside, and J. Zajicek. 1998. Prion immunoreactivity in appendix before clinical onset of variant Creutzfeldt-Jakob disease. *Lancet* 352: 703–704.
45. Kimberlin, R. H., and C. A. Walker. 1989. Pathogenesis of scrapie in mice after intragastric infection. *Virus Res.* 12: 213–220.
46. Williams, S. K., R. Fairless, J. Weise, U. Kalinke, W. Schulz-Schaeffer, and R. Diem. 2011. Neuroprotective effects of the cellular prion protein in autoimmune optic neuritis. *Am. J. Pathol.* 178: 2823–2831.
47. Aude-Garcia, C., C. Villiers, S. M. Candéias, C. Garrel, C. Bertrand, V. Collin, P. N. Marche, and E. Jouvin-Marche. 2011. Enhanced susceptibility of T lymphocytes to oxidative stress in the absence of the cellular prion protein. *Cell. Mol. Life Sci.* 68: 687–696.
48. Rovis, T. L., and G. Legname. 2014. Prion protein-specific antibodies-development, modes of action and therapeutics application. *Viruses* 6: 3719–3737.
49. Heegaard, P. M., A. L. Bergström, H. G. Andersen, and H. Cordes. 2015. Prion-specific antibodies produced in wild-type mice. *Methods Mol. Biol.* 1348: 285–301.
50. Didonna, A., A. C. Venturini, K. Hartman, T. Vranac, V. Čurin Šerbec, and G. Legname. 2015. Characterization of four new monoclonal antibodies against the distal N-terminal region of PrP(c). *PeerJ* 3: e811.
51. Sadowski, M. J., J. Pankiewicz, F. Prelli, H. Scholtzova, D. S. Spinner, R. B. Kascsak, R. J. Kascsak, and T. Wisniewski. 2009. Anti-PrP Mab 6D11 suppresses PrP(Sc) replication in prion infected myeloid precursor line FDC-P1/22L and in the lymphoreticular system in vivo. *Neurobiol. Dis.* 34: 267–278.
52. Mead, S., A. Khalili-Shirazi, C. Potter, T. Mok, A. Nihat, H. Hyare, S. Canning, C. Schmidt, T. Campbell, L. Darwent, et al. 2022. Prion protein monoclonal antibody (PRN100) therapy for Creutzfeldt-Jakob disease: evaluation of a first-in-human treatment programme. *Lancet Neurol.* 21: 342–354.
53. Ferris, R. L., H. J. Lenz, A. M. Trotta, J. García-Foncillas, J. Schulten, F. Audhuy, M. Merlano, and G. Milano. 2018. Rationale for combination of therapeutic antibodies targeting tumor cells and immune checkpoint receptors: harnessing innate and adaptive immunity through IgG1 isotype immune effector stimulation. *Cancer Treat. Rev.* 63: 48–60.
54. Taschuk, R., J. Van der Merwe, K. Marciniuk, A. Potter, N. Cashman, P. Griebel, and S. Napper. 2015. In vitro neutralization of prions with PrP(Sc)-specific antibodies. *Prion* 9: 292–303.
55. Lunnon, K., J. L. Teeling, A. L. Tutt, M. S. Cragg, M. J. Glennie, and V. H. Perry. 2011. Systemic inflammation modulates Fc receptor expression on microglia during chronic neurodegeneration. *J. Immunol.* 186: 7215–7224.
56. Féraudet-Tarisse, C., O. Andréoletti, N. Morel, S. Simon, C. Lacroux, J. Mathey, P. Lamourette, A. Relaño, J. M. Torres, C. Créminon, and J. Grassi. 2010. Immunotherapeutic effect of anti-PrP monoclonal antibodies in transmissible spongiform encephalopathy mouse models: pharmacokinetic and pharmacodynamic analysis. *J. Gen. Virol.* 91: 1635–1645.
57. Prusiner, S. B., D. Groth, A. Serban, R. Koehler, D. Foster, M. Torchia, D. Burton, S. L. Yang, and S. J. DeArmond. 1993. Ablation of the prion protein (PrP) gene in mice prevents scrapie and facilitates production of anti-PrP antibodies. *Proc. Natl. Acad. Sci. USA* 90: 10608–10612.
58. Preithner, S., S. Elm, S. Lippold, M. Locher, A. Wolf, A. J. da Silva, P. A. Baeuerle, and N. S. Prang. 2006. High concentrations of therapeutic IgG1 antibodies are needed to compensate for inhibition of antibody-dependent cellular cytotoxicity by excess endogenous immunoglobulin G. *Mol. Immunol.* 43: 1183–1193.
59. Solomon, B., R. Koppel, E. Hanan, and T. Katzav. 1996. Monoclonal antibodies inhibit in vitro fibrillar aggregation of the Alzheimer beta-amyloid peptide. *Proc. Natl. Acad. Sci. USA* 93: 452–455.
60. Schenk, D., R. Barbour, W. Dunn, G. Gordon, H. Grajeda, T. Guido, K. Hu, J. Huang, K. Johnson-Wood, K. Khan, et al. 1999. Immunization with amyloid-beta attenuates Alzheimer-disease-like pathology in the PDAPP mouse. *Nature* 400: 173–177.
61. Valera, E., B. Spencer, and E. Masliah. 2016. Immunotherapeutic approaches targeting amyloid-β, α-synuclein, and tau for the treatment of neurodegenerative disorders. *Neurotherapeutics* 13: 179–189.
62. Vandenberghe, R., J. O. Rinne, M. Boada, S. Katayama, P. Scheltens, B. Vellas, M. Tuchman, A. Gass, J. B. Fiebach, D. Hill, et al.; Bapineuzumab 3000 and 3001 Clinical Study Investigators. 2016. Bapineuzumab for mild to moderate Alzheimer's disease in two global, randomized, phase 3 trials. *Alzheimers Res. Ther.* 8: 18.
63. Kim, C., T. Haldiman, K. Surewicz, Y. Cohen, W. Chen, J. Blevins, M. S. Sy, M. Cohen, Q. Kong, G. C. Telling, et al. 2012. Small protease sensitive oligomers of PrPSc in distinct human prions determine conversion rate of PrP(C). *PLoS Pathog.* 8: e1002835.
64. Castle, A. R., and A. C. Gill. 2017. Physiological functions of the cellular prion protein. *Front. Mol. Biosci.* 4: 19.
65. Chiesa, R. 2015. The elusive role of the prion protein and the mechanism of toxicity in prion disease. *PLoS Pathog.* 11: e1004745.
66. Jarosz-Griffiths, H. H., N. J. Corbett, H. A. Rowland, K. Fisher, A. C. Jones, J. Baron, G. J. Howell, S. A. Cowley, S. Chintawar, M. Z. Cader, et al. 2019. Proteolytic shedding of the prion protein via activation of metallopeptidase ADAM10 reduces cellular binding and toxicity of amyloid-β oligomers. *J. Biol. Chem.* 294: 7085–7097.
67. Endres, K., G. Mitteregger, E. Kojro, H. Kretzschmar, and F. Fahrenholz. 2009. Influence of ADAM10 on prion protein processing and scrapie infectiosity in vivo. *Neurobiol. Dis.* 36: 233–241.
68. Guhl, S., M. Babina, A. Neou, T. Zuberbier, and M. Artuc. 2010. Mast cell lines HMC-1 and LAD2 in comparison with mature human skin mast cells–drastically reduced levels of tryptase and chymase in mast cell lines. *Exp. Dermatol.* 19: 845–847.
69. Robert, X., and P. Gouet. 2014. Deciphering key features in protein structures with the new ENDscript server. *Nucleic Acids Res.* 42: W320–W324.